PERGAMON

International Journal of Heat and Mass Transfer 44 (2001) 3709–3719

International Journal of HEAT and MASS TRANSFER

www.elsevier.com/locate/ijhmt

Near wake of a circular cylinder submitted to blowing – II Impact on the dynamics

L. Mathelin, F. Bataille, A. Lallemand *

[a] *Institut National des Sciences Appliquées de Lyon, Centre de Thermique de Lyon, UMR 5008, Bât. S. Carnot, 20 Avenue Albert Einstein, 69621 Villeurbanne Cedex, France*

Received 20 July 2000; received in revised form 23 November 2000

Abstract

The near wake of a porous circular cylinder in cross-flow submitted to blowing through its whole surface is experimentally studied. The blowing impact on the Strouhal number exhibits a linear decrease of the vortex shedding frequency with the blowing ratio. A simple model representing this decrease as a function of the injection rate is developed, based on the wake static pressure profile evolution. The main flow temperature influence is also investigated in case of non-isothermal blowing and is shown to have no effect on the Strouhal number evolution. Finally, the interaction between the blowing and the shear layer is investigated through a spectral analysis of the velocity signal. A modification of the shear layer power spectrum is observed when injection occurs. The dynamics are slowed down and characteristic patterns, denoted sub-peaks, appear while the relationship between the von Kármán and the shear layer frequencies without blowing remains valid.

1. Introduction

Bluff body flow is a widely studied problem since the pioneer works of Strouhal in 1878 [1] who observed vortex shedding from a cylinder. In spite of its apparent simplicity, the circular cylinder in cross-flow features most of the phenomena that can be found in bluff bodies wakes, including vortex shedding, boundary layer separation, shear layers and recirculating flows. Von Kármán [2] focused on the vortex street that forms downstream of the cylinder. He found that it was a particularly stable phenomenon and derived a criterion for its existence based on point vortices subjected to small local periodic perturbations analysis. Since then, many investigators have shed light on intrinsic characteristics such as the Strouhal–Reynolds number relationship, base pressure coefficient, shear layer dynamics, end effects, etc. See [3] for a comprehensive review of all these results. More recently, several authors focused on the onset of three-dimensionality in the near wake at low Reynolds numbers. In the last ten years, different three-dimensional aspects have been experimentally addressed, giving a new impulse to the research on bluff bodies. Some three-dimensional instabilities, denoted mode A and mode B, have been identified to be an intrinsic feature of the wake of a circular cylinder at low Reynolds numbers [4–9]. The vortex dislocations and oblique shedding were discovered [10–12] and the role of end effects was clarified [6,13–16]. Williamson [17], as well as Roshko [18], provide the reader with a rich review of these recently discovered three-dimensional phenomena.

In addition to the von Kármán vortex shedding, Bloor [19] found a secondary instability taking place in the separated shear layer. Its relationship with the Reynolds number has received interest from several authors [20–24] but a relatively large discrepancy still exists on the results. Very few studies are concerned with the shear layer modification due to injection.

Besides the experimental studies, powerful computation resources now allow accurate numerical simulations of the two-dimensional and three-dimensional flows around a cylinder to appear. Most of the phenomena cited above have been found through numerical

* Corresponding author. Tel.: +33-4-72-43-8232; fax: +33-4-7243-6010.

E-mail address: a.lal@cethil.insa-lyon.fr (A. Lallemand).

0017-9310/01/$ - see front matter
PII: S0017-9310(01)00021-7

Nomenclature

dx	elementary streamwise length
dy	elementary transverse length
D	cylinder outer diameter
f	frequency
F	blowing rate $((\rho_{inj} U_{inj})/(\rho_\infty U_\infty))$
$\overrightarrow{F}$	force vector
K	constant
l	pressure flat bandwidth
m	mass
n	exponent value in the f_{SL}/f_K relationship
P	static pressure
Re	Reynolds number $(\rho_\infty U_\infty D/\mu_\infty)$
Sr	Strouhal number (fD/U_∞)
T	temperature
T_{band}	motion period associated with the flat band
T_{edge}	motion period associated with one pressure edge
U	fluid velocity magnitude
w	pressure edge width
x	streamwise coordinate
y	transverse coordinate

Greek symbols

α	constant
$\overrightarrow{\gamma}$	acceleration vector
μ	fluid dynamic viscosity
ρ	fluid density

Subscripts

0	no-blowing case
c	critical state (onset of vortex shedding)
e	pressure edge
eq	equivalent Reynolds number
∞	upstream properties
inj	injected fluid
sat	saturation state
SL	shear layer

simulations as well [25–29], giving a strong evidence of the simulation growing capabilities.

Flow control has also received a great deal of work for a few years. It can be achieved by several means such as an intrusive obstacle at an appropriate location in the wake [30], heating the cylinder surface to change the local properties of the flow [31,32], forced cylinder oscillations [33–36], localized blowing or suction [22,37–41]. These techniques allow to shift or suppress the vortex shedding frequency, increase the two-dimensionality of the wake, reduce the sound intensity generated and avoid untimely boundary separation. Nevertheless, injection has been mainly studied for drag reduction purposes through the pioneer works of Wood [42] and Bearman [43]. Their geometry is that of an airfoil profile with a secondary stream flowing through the bluff base and they studied the influence of the bleed coefficient on the drag and the vortex shedding frequency.

The comprehension of the unstable nature of the flow behind a bluff body has also been addressed through a theoretical point of view. After it was developed for plasmas dynamics [44,45], the linear instability theory was successfully applied to fluid mechanics through the work of Koch [46]. It has become a very popular research area and brought new insights for the comprehension of certain phenomena. Based on the time-averaged velocity profile in the near wake of a circular cylinder, the stability criteria can be studied and the vortex shedding frequency estimated. This allows the extension of the study to flow around a bluff body when blowing occurs, provided the time-averaged velocity profile in the near wake is available, either experimentally or numerically. This has been done for a blunt airfoil with base bleed [47–49] but still few studies seem to have been performed on the behavior of the cylinder wake evolution with complete blowing, in particular in non-isothermal cases.

After a brief study of the static pressure evolution in the near wake in Section 2, the primary instability is addressed in Section 3 and a correlation is proposed. In Section 4, a theoretical model, based on results from Section 2, is derived and describes the Strouhal number evolution with blowing. The shear layer dynamics is finally studied in Section 5.

2. The pressure wake

The effect of the blowing has been investigated in the near wake of the cylinder. The modification of the boundary layers thickness (cf. Part I) is expected to strongly influence the development of the von Kármán street and to affect the wake properties. In Fig. 1, the static pressure distribution is plotted for a 29 mm outer diameter porous cylinder at a Reynolds number of 18 700 and $x/D = 1.7$ along the transverse direction y for different blowing rates. Without blowing, it exhibits a typical wake pressure defect. Considering the sharp change of pressure slope as the edge of the wake, its width is about 2.0 D. When blowing occurs, the width is larger, which is consistent with the increasing apparent cylinder diameter. For a 1% injection rate, the width rises to 2.4 D and to 3.2 D for 5.6%. This widening of the wake is accompanied by a decrease in the static pressure defect, leading to the conclusion that the blowing tends to fill the depression at the rear of the cylinder. The results will be supported in Section 4 by the study of the

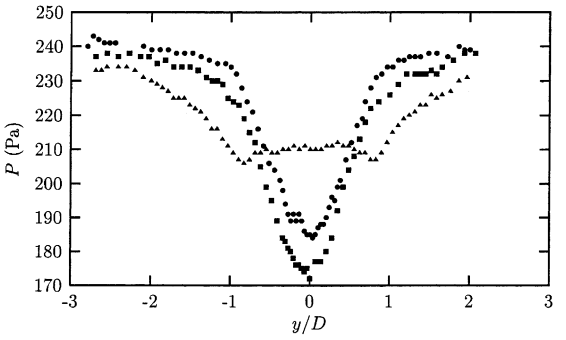

Fig. 1. Transverse static pressure profile in the near wake. $x/D = 1.5$, $Re = 14\,000$. ●, $F = 0\%$; ■, $F = 1.0\%$; ▲, $F = 5.6\%$.

blowing influence on the von Kármán frequency and will lead to a further analysis.

3. Primary instability

Details on the wind-tunnel and measurement techniques can be found in part I. The hot-wire probe cut-off frequency, at least 3 kHz, is not an influencing parameter as the vortex shedding signal is strong enough to be accurately resolved and low compared to 3 kHz. This allows reliable von Kármán and shear layer frequencies records. A third-order low-pass and first-order high-pass Butterworth type frequency filter is applied to prevent a spurious peak in the power spectra to occur from the Fourier transform. Owing to the 65 280 points typically sampled at 6 kHz, the frequency resolution is high enough to consider that the Strouhal number uncertainty is the same as that for the Reynolds number (i.e. 5.5%).

The effect of blowing on the global instability was investigated through a spectral analysis of the signal delivered by a single hot wire probe located in the near wake. The position of the probe is not a crucial parameter as the primary frequency, rising from the Bénard–von Kármán instability, is uniform throughout the whole field. Meanwhile, depending on the probe position, harmonics and sub-harmonics can appear in the velocity signal. For each experimental condition, a Fourier transform of the velocity signal record is performed. The main frequency is then determined using a peak search algorithm on the power spectrum. Experiments were conducted for both isotherm and non-isothermal cases. The Reynolds number was varied from 3900 to 31 000 and the blowing rate from 0% up to 20%. The sampling frequency was chosen so that it is, at least, six times the estimated von Kármán frequency but it was 10 times typically.

When blowing becomes important, the vortex shedding velocity amplitude in the wake and the strength of the von Kármán vortices decrease. This phenomenon is illustrated in Figs. 2 and 3, where the power spectrum of the velocity signal is plotted for $F = 0$ and 8%, respectively, at $Re = 14\,600$. No direct comparison of the absolute power level can be made between the two cases because of the modification of the flow configuration and velocity due to the blowing. The power scale can be considered to have an arbitrary origin and thus only relative level comparisons can be made. The power of the peak corresponding to the vortex shedding frequency decreases with the blowing while it is shifted towards lower frequencies. The general shape of the von Kármán peak remains essentially the same and no additional features appear.

For a certain amount of blowing, the vortex shedding can be totally suppressed, i.e. the von Kármán peak cannot be distinguished from the baseline of the spectrum. One can question whether the vortex shedding phenomenon is gradually suppressed or not. Experiments carried-out for higher blowing rates demonstrate

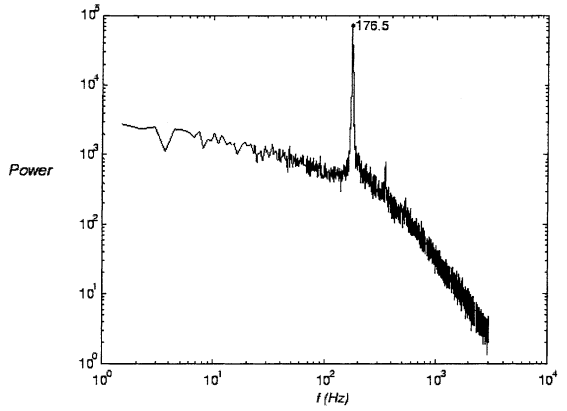

Fig. 2. Velocity magnitude power spectrum in the wake. $x/D = 5$, $y/D = 0.5$, $F = 0\%$, $Re = 14\,600$.

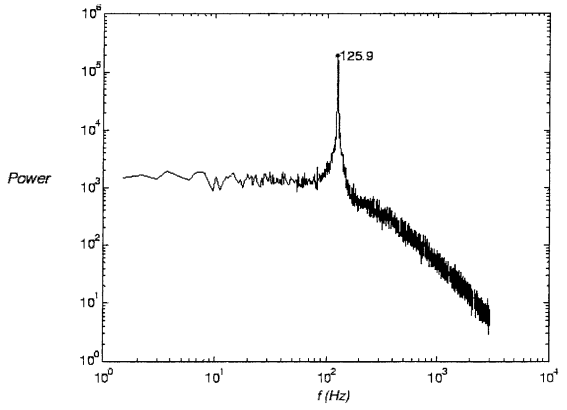

Fig. 3. Velocity magnitude power spectrum in the wake. $x/D = 5$, $y/D = 0.5$, $F = 8\%$, $Re = 14\,600$.

that the vortex shedding mode growth rate gradually decreases with blowing, until it is too weak to sustain regular shedding. The power spectra exhibit a lower and lower von Kármán peak amplitude when blowing is increased. No critical value for the injection rate is proposed due to difficulties in an accurate determination.

The primary instability is studied in terms of Strouhal number, Sr, defined as a non-dimensional vortex shedding frequency:

$$Sr = \frac{f_K D}{U_\infty},$$

where f_K is the vortex shedding frequency and U_∞ the mainstream velocity. Fig. 4 shows the evolution of the Strouhal number with the blowing rate at $Re = 3900$. Sr decreases approximately linearly with the blowing, at least for weak injection rates, and tends to a limit for high rates. This linear evolution is in agreement with a theoretical analysis on the unsteady boundary layer upstream to the separation point [50] though not predicting the slope value. From Fig. 4, it can be noted that Sr is approximately 0.20 in the no-blowing case and decreases to 0.15 for a 5% injection. It corresponds to a 0.75 ratio of the shedding frequency. A test series where the end plates angle relative to the upstream flow direction was varied from 0° to 20° outwards, showed that the use of end plates has no influence on the slope.

Fig. 5 shows the evolution of the Strouhal number with blowing for different Reynolds numbers. For the sake of convenience, the Strouhal numbers have been normalized with the no-blowing value. The slope of the Sr/Sr_0–F curve remains the same for all the Reynolds numbers investigated, keeping a linear decrease with blowing for moderate injection rates. For high F, i.e. roughly $F > 10\%$, the Sr/Sr_0–F relationship is no more linear and asymptotically tends to reach what could be called a saturation state where the Strouhal number hardly decreases with the blowing ratio.

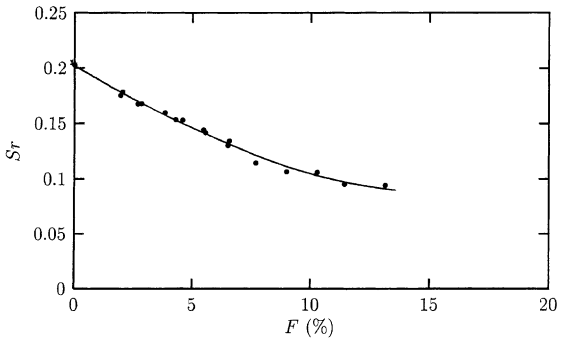

Fig. 4. Evolution of the Strouhal number with blowing, $Re = 3900$.

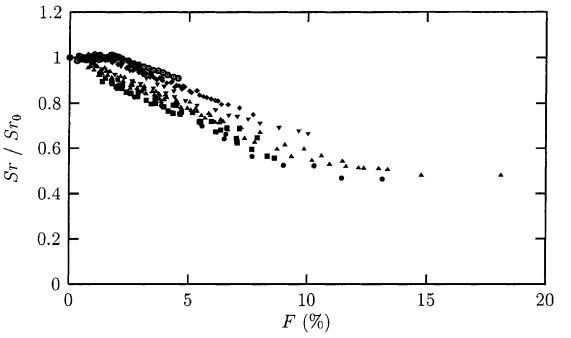

Fig. 5. Evolution of the normalized Strouhal number with blowing. •, $Re = 3900$; ■, $Re = 6300$; ▲, $Re = 9000$; ◆, $Re = 13\,200$; ×, $Re = 21\,000$; +, $Re = 31\,000$.

The dependance of the Strouhal number on the Reynolds number only lies in the appearance of a threshold on the curve when the blowing parameter is increased. It seems that the frequency decrease cannot be initiated below a certain amount of blowing, which increases with the Reynolds number. Extensive experiments were conducted to determine whether this threshold results from a pure end effect or not. Preliminary tests were conducted to study the von Kármán frequency dependance on end plates presence and configuration. It was observed that the threshold tends to decrease, without disappearing, when two-dimensionality is increased, leading to the conclusion that pure end effects only play a minor role. An additional argument could be that for a same degree of two-dimensionality in the wake, the cylinder aspect ratio requirement decreases when the Reynolds number increases [16]. Here, the threshold increases with Re, which should not be the case if it was solely due to pure end effects. One could also think that the blowing tends to lower the three-dimensionality of the near wake. As two-dimensional flows have a higher Strouhal number [7,26,28], one could suggest that the threshold corresponds to the amount of blowing required for the flow to become two-dimensional before the Strouhal number begins to decrease due to the blowing effect itself. This is consistent with the fact that the threshold decreases when the two-dimensionality is artificially promoted with the use of end plates. The amount required is then less important. The threshold would thus be induced from flow three-dimensionality rather than from pure end effects. Typically, the threshold appears around a Reynolds number of 10 000 and increases with Re. Finally, the flow temperature has been proved to have no influence on the threshold presence.

The literature provides results in same tendency as our own experimental works, even if the blowing is here applied on the whole surface of the bluff body, but no direct comparison can be made because of differences in

the geometry. Many authors have experimentally reported a Strouhal number decrease for bluff bodies when base bleed is applied [42,43] or with localized blowing [41,51,52]. These results have also been found using the linear instability theory [48,49,53]. This decrease in the shedding frequency is due to the modification of the time-averaged wake profiles shape, thus changing the value of the complex coefficients in the Ginzburg–Landau equation, leading to a decrease of the most amplified frequency. A complementary interpretation to the modification of the Ginzburg–Landau coefficients could be that the blowing tends to push away the vortices, thus lengthening the formation region at the back of the cylinder. Since Triantafyllou et al. [47], this region is known to be absolutely unstable and it is consistent that its extension modifies the stability pattern and thus the most amplified frequency. In particular, Chomaz et al. [54] showed, through a local stability analysis, that the absolutely unstable region at the rear back of a cylinder must be of finite extent for the flow to develop a global absolute instability and to degenerate into vortex shedding. A modification of the size and location of this region is expected to affect the selected frequency. Pushing the argument even further, if the formation region is pushed away far enough, no more absolute instability region exists in the vicinity of the rear back of the cylinder and the von Kármán vortex street, i.e. the global mode, should disappear. The existence of a critical value for the blowing ratio, above which the vortex shedding no more exists, has also been confirmed by experimental [49,52] and numerical studies [48,53,55].

Finally, we investigated the temperature effect on the Strouhal number evolution with blowing. When the main temperature is varied from ambient temperature to 200°C, while the blown air remains at ambient temperature, the Strouhal–Reynolds number relationship is not modified, demonstrating that it is not dependent on the main to secondary flow temperature ratio. This indicates that the blowing parameter, as defined previously, correctly quantifies the impact of the blowing on the instability frequency and represents the correct definition of the control parameter.

Taking into account the experimental results on the reduction of the Strouhal number with blowing, we developed a relation based on the well-known *Sr–Re* curve [7] given in Fig. 6 to reflect the blowing impact on the flow without blowing. For $Re > 50$, the Strouhal number increases with the Reynolds number, whereas it becomes almost constant and equal to 0.2 for higher Reynolds numbers (beyond 300). The length of the formation region tends to increase in case of blowing and is known to be directly related to the vortex shedding frequency according to the relation $f_K L =$ a constant, where L denotes here the length of the formation region. A lower shedding frequency and a longer formation region correspond to the same effect as a reduction of the flow Reynolds number. Consequently, as the Strouhal number decreases with the blowing, the impact of the blowing on the flow around the cylinder can be seen as a reduction of the wake Reynolds number. The flow submitted to blowing would have the same characteristics, in terms of instability, as a flow associated to a lower Reynolds number without blowing. The impact of the blowing corresponds to a variation along the *Sr–Re* curve, including a reduction of the three-dimensional effects. Consequently, the blowing can be seen as an actor which tends to take back the flow to be two-dimensional.

According to these remarks, we derived a relation to predict the equivalent Reynolds number (Re_{eq}), which corresponds to a flow without injection but with the same value of Strouhal number. The first step, in the derivation of this relation, does not take into account the threshold which occurs for high Reynolds numbers when blowing is applied. According to Figs. 4 and 6, we postulate a relation of the following form

$$Re_{eq} = Re_{sat} + K(1 - e^{-\alpha F}), \tag{1}$$

where Re_{sat} is the Reynolds number at which Sr reaches a constant value ($Sr \simeq 0.2$), K and α are some constants. Considering that the Strouhal number becomes constant for Reynolds numbers higher than 300 and that the critical Reynolds (Re_c) is equal to 50 and using the relation for a very high F, where the Re_c is supposed to be attained, we obtain $K = Re_c - Re_{sat} = 50 - 300 = -250$.

Using results from Fig. 4, we derive the value of 0.5 for α, leading to the final relation

$$Re_{eq} = 300 - 250(1 - e^{-F/2}). \tag{2}$$

This relation allows to easily account for the blowing, giving the characteristics of the flow subjected to injection and the expected Strouhal number, which is then correlated to the modified Reynolds number.

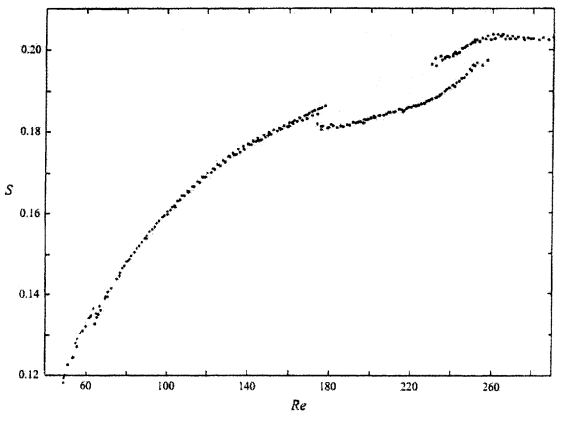

Fig. 6. *Sr–Re* number relationship for low Reynolds numbers. From [7].

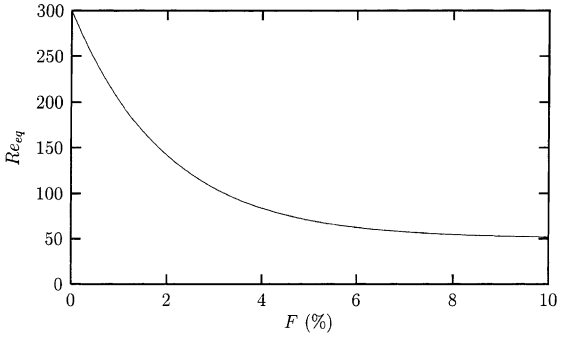

Fig. 7. Equivalent Reynolds number as a function of the blowing ratio for $Re = 3900$.

Fig. 7 exhibits the equivalent Reynolds number for various blowing ratii and a Reynolds number of 3900. With the use of Fig. 6, the Strouhal number value can be estimated knowing that $Sr \simeq 0.2$ for Reynolds numbers higher than 300.

4. Qualitative model for predicting the Strouhal number evolution

Reminding the results presented in Section 2 concerning the static pressure defect profile in the near wake of the cylinder, a qualitative model can be derived. It is thought that the primary frequency, i.e. the vortex shedding frequency, is directly related to the transverse pressure gradient. Keeping in mind the U-shaped profile, one can consider a particle slipping along the wake, while oscillating from one side to the other. With very little physics and mathematics, it is possible to derive an expression for the motion of this particle. Similar types of oscillators models have been proposed in the past (e.g. [56]) based on the wake geometry while many others aim to find appropriate parameters to use in the Strouhal number definition [57–59] for a universal value. Let us assume an infinitely small square particle, whose dimensions are $\mathrm{d}x$ and $\mathrm{d}y$. The particle is submitted to the pressure force but body forces are neglected. The pressure profile considered for modeling is symmetric, consisting in a U-shape whose sharp edges are linear and separated by a flat, i.e. constant, pressure band (see schematic in Fig. 8). Applying the fundamental law of mechanics, $\overrightarrow{F} = m\overrightarrow{\gamma}$, it follows

$$\frac{\partial P}{\partial y}\mathrm{d}x\,\mathrm{d}y = -\rho\,\mathrm{d}x\,\mathrm{d}y\ddot{y}. \tag{3}$$

Dotted letter denotes its time derivative. The starting point, for $t = 0$, is assumed to be $y = w + l/2$ and $\dot{y} = 0$, where l is the flat bandwidth and w the "edge depth". To find the period associated with this configuration, the flat band and the edge problems are separately treated.

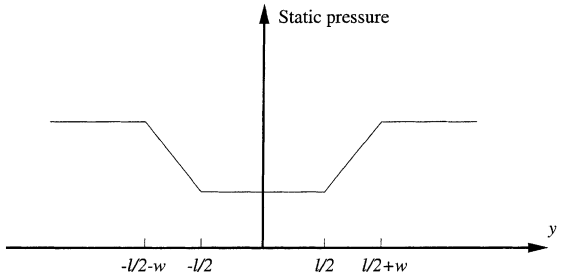

Fig. 8. Schematic of the pressure wake model.

First, only one edge is considered to act on the particle and the flat band is not accounted. Next, edge model results are used to derive the period associated to the flat band only.

The motion period or time required for the particle to slip along one edge is, after little mathematics,

$$T_{\mathrm{edge}} = \sqrt{\frac{2\rho w}{|\partial P/\partial y|_{\mathrm{e}}}}, \tag{4}$$

where $|\partial P/\partial y|_{\mathrm{e}}$ is the mean pressure gradient at the edge. To calculate the period associated with the flat band, one needs the particle velocity at $y = l/2$. It reads

$$|\dot{y}(l/2)| = \sqrt{\frac{2w|\partial P/\partial y|_{\mathrm{e}}}{\rho}}. \tag{5}$$

Then, the period associated to the flat band is simply

$$T_{\mathrm{band}} = 2l\sqrt{\frac{\rho}{2w|\partial P/\partial y|_{\mathrm{e}}}}. \tag{6}$$

Finally, the vortex shedding period is assumed to be the period of oscillation of the particle from one side to the other, i.e. the sum of twice the time required for the particle to cross the flat band added of four times the time for slipping along one edge. Expressed in terms of Strouhal number, one gets

$$Sr = \frac{D}{U_\infty}\sqrt{\frac{w|\partial P/\partial y|_{\mathrm{e}}}{2\rho(16w^2 + l^2)}}. \tag{7}$$

This model aims to predict the Strouhal number evolution from the modification of the near wake when blowing occurs. Because of its simplistic hypotheses, especially to consider a linear pressure profile, it is not to be seen as a predictive model for the vortex shedding frequency itself but only to reflect the evolution of the Strouhal number with blowing. Large errors can be induced when estimating the pressure gradient value or the size of the different model characteristics (h and l).

When applied to the static pressure profile presented in Fig. 1, the predicted Strouhal number ratio between the 5.6% injection rate case and the no-blowing case is about 0.63. Using Fig. 5, the experimental ratio reported

is around 0.80, leading to the conclusion that this model gives a rough, while not perfect, estimation of the impact of the blowing on the primary instability frequency. The Strouhal number ratio between no-blowing and 1% injection is found to be about 1.05 to be compared to the experimentally found 1.02 value. This clearly indicates that the threshold in the *Sr–Re* curve studied above also appears in the near wake. Under sufficiently weak blowing, the pressure gradient tends to increase rather than decrease, while the wake width does not increase significantly. This makes the Strouhal number to slightly increase as proved in Fig. 5. The presented model is thus able to account for the threshold effect as well, provided the static pressure profile is available.

5. Shear layer instability

For particular probe positions, the Fourier spectra obtained for the determination of the von Kármán frequency exhibit a secondary peak relevant to what is often referred in the literature as the "transition waves" [19] or secondary vortices [21]. This secondary instability arises from the separated shear layer due to mechanisms similar to that of the formation of the Kelvin–Helmholtz vortices in a free shear layer or Tollmien–Schlichting vortices for a boundary layer. It has long been shown that the shear layer frequency, hereafter denoted f_{SL}, can be expressed as a function of the Reynolds number and the von Kármán frequency f_K of the form $f_{SL}/f_K \sim Re^n$ [19,21–24,60]. A large discrepancy about the n coefficient value is observed in the literature as Bloor [19] found a $Re^{1/2}$ relationship between secondary and primary instability frequencies ($n = 0.5$), while Wei and Smith [21] found $n = 0.87$ for a Reynolds number ranging from 1200 to 11 000. Compiling all the available data and based on theoretical considerations, Prasad and Williamson [23] finally proposed a 0.67 value for n.

In this part, the study is focused on the modification of the shear layer dynamics in case of blowing. In particular, the Fourier analysis will give insights into the spectral energy distribution. Here again, the probe position is of no importance, as long as it is in the shear layer, for the determination of this frequency. The probe was typically located at $x/D = 0.5$ and $y/D = 0.6$.

Applying the same criterion as for the Strouhal number measurement, the sampling frequency was typically set to 6 kHz, acquiring 262 000 points. Third-order low-pass filter was applied to cut off the signal bandwidth, thus preventing spurious peaks to occur from the Fourier transform. The Fourier transform is typically proceeded on 16 384-point ensemble-averaged blocks to ensure low noise. The blocks size allows for a 0.4 Hz frequency resolution and low noise on the spectral signal. First experiments were conducted without blowing, thus providing a reference basis for comparison with literature. An example of power spectrum obtained for $Re = 5400$ is shown in Fig. 9. The sharp high first peak corresponds to the von Kármán frequency, while sub- and higher harmonics are present. The broad peak reveals the shear layer instability and the f_{SL} value is taken as the frequency of the top of the "hump". The width of these peaks reveals the nature of their instability. Absolute instability exhibits a very sharp peak as for the von Kármán shedding, while a convective instability has a broad distribution (shear layer). Fitting our f_{SL} measures in the no-blowing case, not plotted here for sake of brevity, we found $n = 0.64$, in good agreement with the $n = 0.67$ value proposed by Prasad and Williamson [23].

When blowing is applied, both the von Kármán and the shear layer peaks move left towards lower frequencies as can be seen in Fig. 10. As shown by Bloor [19], the f_{SL} mainly scales with the velocity outside the boundary layer at the separation point and the corresponding momentum thickness leading to an $f_{SL} \sim U_{outside}/\theta_s$ relationship, where θ_s is the momentum thickness of the separated shear layer. Blowing thickens the boundary layer and increases the momentum thickness of the shear layer. Velocity outside the boundary layer at the separation point is not thought to radically change when blowing occurs, even if the separation angle is slightly promoted. Following this, it comes that f_{SL} should decrease with blowing. Fig. 11 shows the evolution of the secondary to primary frequency ratio with blowing as a function of the Reynolds number. The f_{SL}/f_K relationship proposed by Prasad and Williamson [23] is also plotted for comparison. It is clear that the present data with blowing match rather accurately this relationship. Regression of the curve leads again to a 0.64 coefficient. Consequently, the blowing seems to

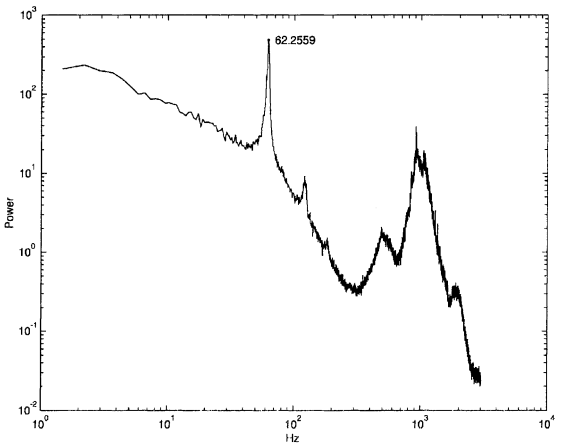

Fig. 9. Velocity magnitude power spectrum in the shear layer. $x/D = 0.5$, $y/D = 0.6$, $Re = 5400$, $F = 0\%$.

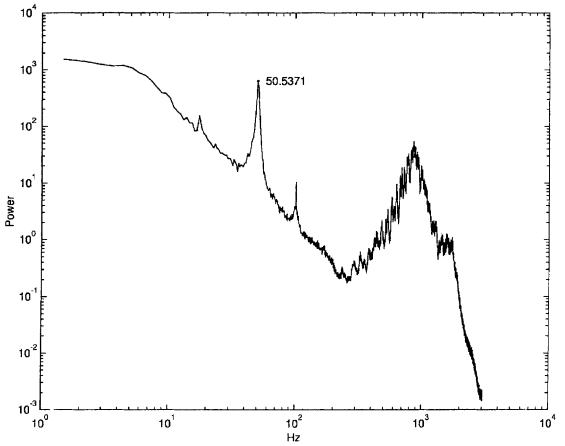

Fig. 10. Velocity magnitude power spectrum in the shear layer. $x/D = 0.5$, $y/D = 0.6$, $Re = 5400$, $F = 4\%$.

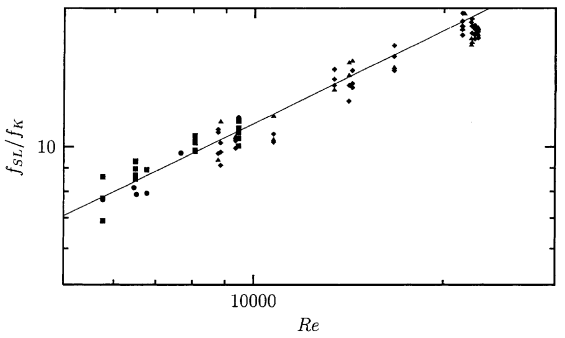

Fig. 11. Secondary to primary instability frequency ratio evolution with the Reynolds number. Symbols refer to different data series. Solid line is the relationship from [23].

similarly act on primary and secondary instabilites, keeping the f_{SL}/f_K relationship valid.

Accurately scrutinizing Fig. 10 where blowing occurs, one can notice the shear layer peak does not look smooth (if one excepts the measurement noise) but seems to be hacked. For comparison convenience, Figs. 12 and 13 show a magnified view of the shear layer power spectrum with and without blowing. Examination of these spectra leads to the conclusion that, in case of blowing, the shear layer peak exhibits what is hereafter denoted "subpeaks". Extensive experiments, with up to more than 10^6 points sampled, as in Figs. 9–11, were carried out to confirm the existence of this phenomenon. Considering the number of points sampled for the Fourier transform, the frequency resolution (0.4 Hz) is high enough to ensure the subpeaks, which successive frequency gaps are comprised between 20 and 40 Hz, are not a dummy phenomenon. When varying the flow conditions, it appears that these subpeaks do not change in position, i.e. their frequencies remain exactly the

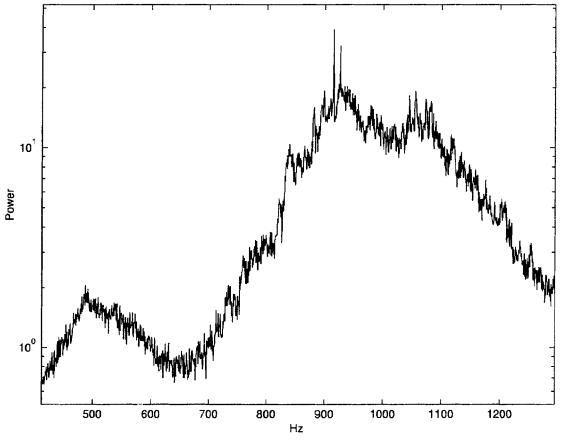

Fig. 12. Detail of the shear layer peak power spectrum. $x/D = 0.5$, $y/D = 0.6$, $Re = 5400$, $F = 0\%$.

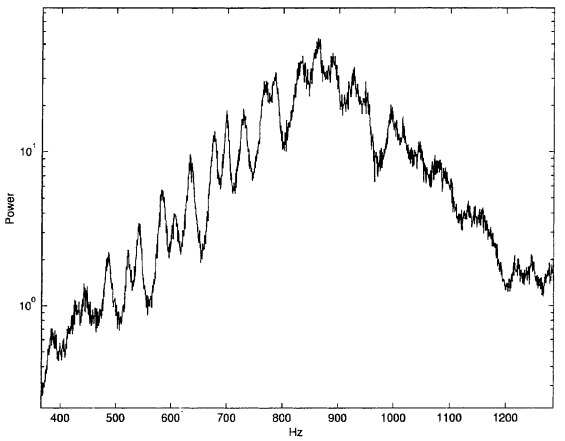

Fig. 13. Detail of the shear layer peak power spectrum. $x/D = 0.5$, $y/D = 0.6$, $Re = 5400$, $F = 4\%$.

same. Their baseline, the shear layer peak envelop, moves with the Reynolds number or the injection rate, but not the subpeaks frequency. Nevertheless, their amplitude follows the evolution of the shear layer peak envelop. It seems that the broad shear layer peak acts as a "spectral window" revealing a spectral subpeaks series. When the windows move, i.e. when blowing occurs or the Reynolds number changes, others subpeaks are visible but the underlying subpeaks "comb" remains the same whatever the blowing ratio. The shear layer instability acts as selective amplifier or revealer.

Because of this insensitivity to any flow condition, one can think about an external independent perturbation. Extensive experiments and verifications have been carried out. The measurement position, the probe type (hot and cold wire), the cylinder diameter, the fan velocity (airfoils frequency), the intrinsic structure

frequency, the end plates configuration, the aspect and blockage ratii, the upstream temperature and velocity, the injection rate, the cylinder porosity, the sampling time length and frequency and the frequential filters value were changed but do not have any influence on the subpeaks frequency. The gap between two successive peaks is not constant and no coherence has been found in its distribution, as should be the case if these peaks were due to a resonance-like phenomenon.

Reminding that these subpeaks do not exist, or at least, are not detectable without blowing, one can think that an interaction between the secondary and the primary flow occurs. This interaction would take place just beyond the boundary layer separation from the cylinder, in the shear layer. The blown flow could interact with the Kelvin–Helmholtz vortices chain present in the shear layer and create the source of the perturbations.

6. Conclusions

The impact of the blowing through the porous surface of a circular cylinder in cross-flow on the wake dynamics was experimentally investigated. The wake was proved to widen with blowing, which is consistent with the fact that the apparent cylinder diameter is higher. The wake static pressure defect decreases with the blowing, due to the net injected mass into the flow.

The study also emphasized the modification of the stability patterns. The Strouhal number, linearly related to the vortex shedding frequency in the von Kármán street, was investigated under various blowing conditions. It decreases with the injection ratio until a saturation state is reached and no temperature effect in the no-isothermal cases has been exhibited. The decrease is due to the modification of the time-averaged near wake fields (velocity, vorticity and pressure), which induces an evolution of the stability properties. Several ideas have been proposed for the impact of the blowing on the stability patterns. Furthermore, a relation giving an equivalent Reynolds number of the flow submitted to blowing was derived.

A model was proposed to estimate the vortex shedding frequency from the time-averaged wake static pressure profile. It is suggested that this frequency is strongly dependent on the transverse pressure gradient. Satisfying agreement was found between experimental data and values computed from the model.

Finally, the secondary instability, which develops within the shear layer is proved to be influenced by blowing as well. Its intrinsic features remain the same but its most amplified frequency decreases. The f_K/f_{SL} relationship proposed by Prasad and Williamson [23] is proved to remain valid. What could be a blowing interaction with the Kelvin-Helmholtz vortices, which develop in the shear layer, was exhibited. This interaction is revealed through subpeaks appearing in the shear layer peak power spectrum when blowing occurs.

References

[1] V. Strouhal, Ann. Phys. Chem. (Liepzig) Neue Folge 5, Heft 10 (1878) 216–251.
[2] T. von Kármán, On the mechanism of drag generation on the body moving in fluid, in: Nachrichten der Königliche Gesellschaft der Wissenschaften zu Göttigen, 1912, Part I: pp. 509–517; Part II: pp. 547–556.
[3] M.M. Zdravkovich, in: Flow Around Circular Cylinders. Fundamentals, Oxford University Press, Oxford, 1997, p. 672.
[4] C.H.K. Williamson, The existence of two stages in the transition to three-dimensionality of a cylinder wake, Phys. Fluids 31 (11) (1988) 3165–3168.
[5] T. Leweke, M. Provansal, The flow behind rings: bluff body wakes without end effects, J. Fluid Mech. 288 (1995) 265–310.
[6] M. Brede, H. Eckelmann, D. Rockwell, On secondary vortices in the cylinder wake, Phys. Fluids 8 (8) (1996) 2117–2124.
[7] C.H.K. Williamson, Three-dimensional wake transition, J. Fluid Mech. 328 (1996) 345–407.
[8] T. Leweke, C.H.K. Williamson, Three-dimensional instabilities in wake transition, Eur. J. Mech. B/Fluids 17 (4) (1998) 571–586.
[9] R.B. Green, J.H. Gerrard, Vorticity measurements in the near wake of a circular cylinder at low Reynolds numbers, J. Fluid Mech. 246 (1993) 675–691.
[10] C.H.K. Williamson, Oblique and parallel modes of vortex shedding in the wake of a circular cylinder at low Reynolds numbers, J. Fluid Mech. 206 (1989) 579–627.
[11] C.H.K. Williamson, The natural and forced formation of spot-like 'vortex dislocation' in the transition of a wake, J. Fluid Mech. 243 (1992) 393–441.
[12] M. König, H. Eisenlohr, H. Eckelmann, The fine structure in the *Sr–Re* relationship of the laminar wake of a circular cylinder, Phys. Fluids A 2 (1990) 1607–1614.
[13] H. Eisenlohr, H. Eckelmann, Vortex splitting and its consequences in the vortex street wake of cylinders at low Reynolds number, Phys. Fluids A 1 (2) (1989) 189–192.
[14] M. Hammache, M. Gharib, An experimental study of the parallel and oblique vortex shedding from circular cylinders, J. Fluid Mech. 232 (1991) 567–590.
[15] M. König, B.R. Noack, H. Eckelmann, Discrete shedding modes in the von Kármán street, Phys. Fluids A 5 (7) (1993) 1846–1848.
[16] C. Norberg, An experimental investigation of the flow around a circular cylinder: influence of aspect ratio, J. Fluid Mech. 258 (1994) 287–316.
[17] C.H.K. Williamson, Vortex dynamics in the cylinder wake, Annu. Rev. Fluid Mech. 28 (1996) 477–539.
[18] A. Roshko, Perspectives on bluff body aerodynamics, J. Wind Engng. Indust. Aerodyn. 49 (1993) 79–101.
[19] M.S. Bloor, The transition to turbulence in the wake of a circular cylinder, J. Fluid Mech. 19 (1964) 290–304.

[20] J.H. Gerrard, The wakes of cylindrical bluff bodies at low Reynolds number, Philos. Trans. R. Soc. Lond. A 288 (1978) 351–382.
[21] T. Wei, C.R. Smith, Secondary vortices in the wake of circular cylinders, J. Fluid Mech. 169 (1986) 513–533.
[22] J.-C. Lin, J. Towfighi, D. Rockwell, Near-wake of a circular cylinder: control by steady and unsteady surface injection, J. Fluids Struct. 9 (1995) 659–669.
[23] A. Prasad, C.H.K. Williamson, The instability of the shear layer separating from a bluff body, J. Fluid Mech. 333 (1997) 375–402.
[24] J. Mihailovic, T.C. Corke, Three-dimensional instability of the shear layer over a circular cylinder, Phys. Fluids 9 (11) (1997) 3250–3257.
[25] T. Tamura, I. Ohta, K. Kuwahara, On the reliability of two-dimensional simulation for unsteady flows around a cylinder-type structure, J. Wind Eng. Ind. Aerodyn. 35 (1990) 275–298.
[26] R. Mittal, S. Balachandar, Effect of three-dimensionality on the lift and drag of nominally two-dimensional cylinders, Phys. Fluids 7 (8) (1995) 1841–1865.
[27] H.-Q. Zhang, U. Fey, B.R. Noack, M. König, H. Eckelmann, On the transition of the cylinder wake, Phys. Fluids 7 (4) (1995) 779–794.
[28] H. Persillon, M. Braza, Physical analysis of the transition to turbulence in the wake of a circular cylinder by three-dimensional Navier–Stokes simulation, J. Fluid Mech. 365 (1998) 23–88.
[29] Y. Na, P. Moin, Direct numerical simulation of a separated turbulent boundary layer, J. Fluid Mech. 374 (1998) 379–405.
[30] P.J. Strykowski, K.R. Sreenivasan, On the formation and suppression of vortex shedding at low Reynolds numbers, J. Fluid Mech. 218 (1990) 71–107.
[31] T. Masuoka, Y. Takatsu, K. Naganuma, T. Tsuruta, Suppression of the Kármán vortex street by wake heating, in: Proceedings of the 11th International Heat Transfer Conference, vol. 5, Kyongju, Korea, 1998.
[32] R.N. Kieft, C.C.M. Rindt, A.A. van Steenhoven, The influence of buoyancy on the behavior of the vortex structures in a cylinder wake, in: Proceedings of the 11th International Heat Transfer Conference, vol. 6, Kyongju, Korea, 1998.
[33] M. Nishioka, H. Sato, Mechanism of determination of the shedding frequency of vortices behind a cylinder at low Reynolds numbers, J. Fluid Mech. 89 (1978) 49–60.
[34] M. Provansal, C. Mathis, L. Boyer, Bénard–von Kármán instability: transient and forced regimes, J. Fluid Mech. 182 (1987) 1–22.
[35] D. Rockwell, Active control of globally-unstable separated flows, in: Proceedings of the International Symposium on Non-steady Fluid Dynamics, vol. 92, Toronto, Canada, 1990.
[36] F. Nuzzi, C. Magness, D. Rockwell, Three-dimensional vortex formation from an oscillating, non-uniform cylinder, J. Fluid Mech. 238 (1992) 31–54.
[37] T. Hayashi, F. Yoshino, R. Waka, The aerodynamic characteristics of a circular cylinder with tangential blowing in uniform shear flows, JSME Int. J., Ser. B 36 (1) (1993) 101–112.
[38] K. Roussopoulos, Feedback control of vortex shedding at low Reynolds numbers, J. Fluid Mech. 248 (1993) 267–296.
[39] D.S. Park, D.M. Ladd, E.W. Hendricks, Feedback control of von Kármán vortex shedding behind a circular cylinder at low Reynolds numbers, Phys. Fluids 6 (7) (1994) 2390–2405.
[40] M. Amitay, J. Cohen, Instability of a two-dimensional plane wall jet subjected to blowing or suction, J. Fluid Mech. 344 (1997) 67–94.
[41] D.A. Hammond, L.G. Redekopp, Global dynamics of symmetric and asymmetric wakes, J. Fluid Mech. 331 (1997) 231–260.
[42] C.J. Wood, The effect of base bleed on a periodic wake, J. Royal Aero. Soc. (Technical notes) 68 (1964) 477–482.
[43] P.W. Bearman, The effect of base bleed on the flow behind a two-dimensional model with a blunt trailing edge, Aero. Quart. 18 (1967) 207–224.
[44] R.J. Briggs, in: Electron–Stream Interaction with Plasmas, MIT Press, Cambridge, MA, 1964.
[45] A. Bers, Linear waves and instabilities, in: C. DeWitt, J. Peyraud, (Eds.), Physique des Plasmas, Gordon and Breach, London, 1975, pp. 117–213.
[46] W. Koch, Local instability characteristics and frequency determination of self-excited wake flows, J. Sound Vib. 99 (1) (1985) 53–83.
[47] G.S. Triantafyllou, M.S. Triantafyllou, C. Chryssostomidis, On the formation of vortex streets behind stationary cylinders, J. Fluid Mech. 170 (1986) 461–477.
[48] K. Hannemann, H. Oertel Jr., Numerical simulation of the absolutely and convectively unstable wake, J. Fluid Mech. 199 (1989) 55–88.
[49] M. Schumm, E. Berger, P.A. Monkewitz, Self-excited oscillations in the wake of two-dimensional bluff bodies and their control, J. Fluid Mech. 271 (1994) 17–53.
[50] R.D. Cohen, Predicting the effects of surface suction and blowing on the Strouhal frequencies in vortex shedding, JSME Int J. 34 (1) (1991) 30–38 Series II.
[51] M. Morzyński, K. Afanasiev, F. Thiele, Non-parallel flow stability and the wake control problem, Z. Angew. Math. Mech. 78 (1998) S631–S632.
[52] O. Inoue, T. Yamazaki, T. Bisaka, Numerical simulation of forced wakes around a cylinder, Int. J. Heat and Fluid Flow 16 (5) (1990) 327–332.
[53] H. Oertel Jr., Wakes behind blunt bodies, Annu. Rev. Fluid Mech. 22 (1990) 539–564.
[54] J.M. Chomaz, P. Huerre and L.G. Redekopp, Models of hydrodynamics resonance in separated shear flows, in: Proceedings of the Sixth Symposium on Turbulent Shear Flows, Toulouse, France, 1987.
[55] P.A. Monkewitz, L.N. Nguyen, Absolute instability in the near-wake of two-dimensional bluff bodies, J. Fluids Struct. 1 (1987) 165–184.
[56] G. Birkoff, E.H. Zarantello, in: Jets, Wakes and Cavities, Academic Press, New York, 1957.
[57] A. Roshko, On the wake and drag of bluff bodies, J. Aero. Sciences 22 (1955) 124–132.
[58] H.B. Awbi, An assessment of the universal Strouhal number concepts for two-dimensional bluff bodies, Aero. J. (1981) 467–469.

[59] C.H.K. Williamson, G.L. Brown, A series in $1/\sqrt{Re}$ to represent the Strouhal–Reynolds number relationship of the cylinder wake, J. Fluids Struct. 12 (1998) 1073–1085.

[60] A. Kourta, H.C. Boisson, P. Chassaing, H. HaMinh, Nonlinear interaction and the transition to turbulence in the wake of a circular cylinder, J. Fluid Mech. 181 (1987) 141–161.